Electrochemically Controlled Formation and Growth of Hydrogen Nanobubbles

Lijuan Zhang,[†,§] Yi Zhang,[†] Xuehua Zhang,[‡] Zhaoxia Li,[†,§] Guangxia Shen,[†] Ming Ye,[†,§] Chunhai Fan,*[,†] Haiping Fang,*[,†] and Jun Hu*[,†,‡]

Shanghai Institute of Applied Physics, Chinese Academy of Sciences, Shanghai 201800, Bio-X Life Science Research Center, College of Life Science and Biotechnology, Shanghai Jiao Tong University, Shanghai 200030, and Graduate School of the Chinese Academy of Sciences, Beijing 100080, China

Received March 30, 2006. In Final Form: June 5, 2006

Electrogenerated microscale bubbles that are confined at the electrode surface have already been extensively studied because of their significant influence on electrochemistry. In contrast, as far as we know, whether nanoscale bubbles exist on the electrode surface has not been experimentally confirmed yet. Here, we report the observation of electrochemically controlled formation and growth of hydrogen nanobubbles on bare highly oriented pyrolytic graphite (HOPG) surface via in-situ tapping mode atomic force microscopy (TMAFM). By using TMAFM imaging, we observed that electrochemically generated hydrogen gas led to the formation of nanobubbles at the HOPG surface. We then employed a combination of techniques, including phase imaging, ex-situ degassing, and tip perturbation, to confirm the gas origin of such observed nanobubbles. We further demonstrated that the formation and growth of nanobubbles could be well controlled by tuning either the applied voltage or the reaction time. Remarkably, we could also monitor the evolution process of nanobubbles, that is, formation, growth, coalescence, as well as the eventual release of merged microbubbles from the HOPG surface.

Introduction

The influence of electrogenerated gases on electrochemical reactions has historically attracted significant research interest and still remains a challenging topic.[1−4] Since electrochemical reactions occur primarily in aqueous solutions, gases (e.g., hydrogen and oxygen) are usually generated at electrode surfaces. As a result, electrogenerated gases may form bubbles and stick to the electrode surface and significantly affect the electrochemical reaction system.[5,6] For example, Tsai et al. elegantly demonstrated that adsorbed hydrogen bubbles were responsible for bubble-shaped microscale defects, which were often encountered in electrodeposited coatings.[3] More recently, Wang and co-workers observed that water-electrolysis-induced mineralization led to the formation of submicrometer vaterite tubes at the cathode surface, which indirectly suggested the existence of nanoscale bubbles at electrode surfaces.[7] In this work, we present direct evidence that electrochemical generation of hydrogen does induce the formation of hydrogen nanobubbles at the electrode surface.

Nanoscale bubbles at the solid−water interface were first predicted from force measurements[8] in 1994, and their stable existence was recently reported by using atomic force microscopy (AFM).[9−13] Other techniques, including rapid cryofixation-freeze fracture[14] and neutron reflectometry,[15] also suggested the existence of nanobubbles. The existence of nanobubbles has many important implications. In particular, their existence at the hydrophobic solid−liquid interface may significantly change the dynamics of a variety of systems, such as long-ranged interfacial interactions,[8,16] stability of colloidal systems,[17] and reduction of friction and drag in microfluidic transportation.[18,19] Nanobubbles were also suggested to be associated with a wide range of applications such as fast folding of proteins and assembly,[20−22] design of biosensors/biochips,[23] detergent-free cleaning,[24,25] ultrasound diagnostics and local drug delivery in medicine,[26] and design of fluidic microchannels[27] and nanodevices.[28]

* To whom correspondence should be addressed. E-mail: fchh@sinap.ac.cn, fanghaiping@sinap.ac.cn, jhu@sjtu.edu.cn.

† Shanghai Institute of Applied Physics, Chinese Academy of Sciences.

‡ Shanghai Jiao Tong University.

§ Graduate School of the Chinese Academy of Sciences.

(1) Westerheide, D. E.; Westwater, J. W. *AIChE J.* **1961**, *7*, 357−362.
(2) Allongue, P.; Devilleneuve, C. H.; Pinsard, L.; Bernard, M. C. *Appl. Phys. Lett.* **1995**, *67*, 941−943.
(3) Tsai, W. L.; Hsu, P. C.; Hwu, Y.; Chen, C. H.; Chang, L. W.; Je, J. H.; Lin, H. M.; Groso, A.; Margaritondo, G. *Nature* **2002**, *417*, 139−139.
(4) Saraf, L.; Baer, D. R.; Wang, Z. M.; Young, J.; Engelhard, M. H.; Thevuthasan, S. *Surf. Interface Anal.* **2005**, *37*, 555−561.
(5) Weijs, M. P. M. G.; Janssen, L. J. J.; Visser, G. J. *J. Appl. Electrochem.* **1997**, *27*, 371−378.
(6) Boissonneau, P.; Byrne, P. *J. Appl. Electrochem.* **2000**, *30*, 767−775.
(7) Fan, Y.; Wang, R. *Adv. Mater.* **2005**, *17*, 2384−2388.
(8) Parker, J. L.; Claesson, P. M.; Attard, P. *J. Phys. Chem.* **1994**, *98*, 8468−8480.
(9) Lou, S. T.; Ouyang, Z. Q.; Zhang, Y.; Li, X. J.; Hu, J.; Li, M. Q.; Yang, F. J. *J. Vac. Sci. Technol., B* **2000**, *18*, 2573−2575.
(10) Tyrrell, J. W. G.; Attard, P. *Phys. Rev. Lett.* **2001**, *87*, 1761041−1761044.
(11) Attard, P. *Adv. Colloid Interface Sci.* **2003**, *104*, 75−91.
(12) Agrawal, A.; Park, J.; Ryu, D. Y.; Hammond, P. T.; Russell, T. P.; McKinley, G. H. *Nano Lett.* **2005**, *5*, 1751−1756.
(13) Zhang, X. H.; Maeda, N.; Craig, V. S. J. *Langmuir* **2006**, *22*, 5025−5035.
(14) Switkes, M.; Ruberti, J. W. *Appl. Phys. Lett.* **2004**, *84*, 4759−4761.
(15) Steitz, R.; Gutberlet, T.; Hauss, T.; Klosgen, B.; Krastev, R.; Schemmel, S.; Simonsen, A. C.; Findenegg, G. H. *Langmuir* **2003**, *19*, 2409−2418.
(16) Carambassis, A.; Jonker, L. C.; Attard, P.; Rutland, M. W. *Phys. Rev. Lett.* **1998**, *80*, 5357−5360.
(17) Nguyen, A. V.; Evans, G. M.; Nalaskowski, J.; Miller, J. D. *Exp. Therm. Fluid Sci.* **2004**, *28*, 387−394.
(18) Zhu, Y. X.; Granick, S. *Phys. Rev. Lett.* **2001**, *87*, 0961051−0961054.
(19) de Gennes, P. G. *Langmuir* **2002**, *18*, 3413−3414.
(20) Zhou, R. H.; Huang, X. H.; Margulis, C. J.; Berne, B. J. *Science* **2004**, *305*, 1605−1609.
(21) Liu, P.; Huang, X. H.; Zhou, R. H.; Berne, B. J. *Nature* **2005**, *437*, 159−162.
(22) Ball, P. *Nature* **2003**, *423*, 25−26.
(23) Holmberg, M.; Kuhle, A.; Garnaes, J.; Morch, K. A.; Boisen, A. *Langmuir* **2003**, *19*, 10510−10513.
(24) Pashley, R. M.; Rzechowicz, M.; Pashley, L. R.; Francis, M. J. *J. Phys. Chem. B* **2005**, *109*, 1231−1238.
(25) Maeda, N.; Rosenberg, K. J.; Israelachvili, J. N.; Pashley, R. M. *Langmuir* **2004**, *20*, 3129−3137.
(26) Lohse, D. *Phys. Today* **2003**, *56*, 36−39.
(27) Granick, S.; Zhu, Y. X.; Lee, H. *Nat. Mater.* **2003**, *2*, 221−227.
(28) Paxton, W. F.; Kistler, K. C.; Olmeda, C. C.; Sen, A.; St Angelo, S. K.; Cao, Y. Y.; Mallouk, T. E.; Lammert, P. E.; Crespi, V. H. *J. Am. Chem. Soc.* **2004**, *126*, 13424−13431.

10.1021/la060859f CCC: $33.50
Published on Web 07/29/2006

However, given these research efforts and advances, the origin of nanobubbles still remains ambiguous and under debate.[29−33] Of note, most previous experimental results on nanobubbles available in the literature were of conflict as well, which might arise from the influence of many factors such as complicated behavior of hydrophobic self-assembled monolayer surfaces,[34,35] possible experimental artifacts,[29] and dissolved gases.[31,36]

To better understand electrochemical interfaces and settle the above-mentioned nanobubble debate, we focus on the study of formation and existence of hydrogen nanobubbles at highly oriented pyrolytic graphite (HOPG) electrode surfaces under electrochemical control. In fact, de Gennes suggested that high concentration of gases is crucial for their adsorption and probably for the nanobubble formation at the solid−water interface,[19] while electrochemistry is well suited to rapidly generate a large amount of gas molecules, leading to a high local gas concentration proximal to the electrode surface. We also note that the origin of electrochemically generated gases is well defined. For example, in a diluted sulfuric acid solution, only hydrogen gas is generated at sufficiently negative potentials.

Experimental Section

Materials. Water with a conductivity of 18.2 MΩ•cm was obtained from a Milli-Q system (Millipore Corp., Boston, MA). Concentrated sulfuric acid and ethanol (GR grade) were purchased from Chinese Chemical Reagent Co. HOPG (dimension 1.2 × 1.2 cm, ZYA grade, from Mikromasch Co.) served as both the electrochemical electrode and the substrate for the nanobubble. It was mounted on a matching steel shim (Digital Instruments, Santa Barbara, CA) via electric silver epoxy (Shanghai Institute of Synthetic Resin, China). HOPG surface was freshly cleaved by adhesive tapes prior to each experiment. Platinum wires with the diameter of 0.3 mm were purchased from Chinese Boyoubo Co. and served as both auxiliary and quasi-reference electrodes.

Electrochemistry. Electrolysis of water was performed in a pre-degassed diluted sulfuric acid solution (0.01 M). The electrolyte was pre-degassed and then was rapidly injected into the Nanoscope quartz fluid cell. The electrochemical reaction was carried out with a CHI 600B electrochemical workstation (CH Instruments).

Tapping Mode Atomic Force Microscopy (TMAFM) Imaging. TMAFM imaging was performed with a MultiMode Nanoscope IIIa SPM from Digital Instruments (Veeco Metrology Group, NY) at 25 ± 2 °C. NP-S cantilever (0.58 N/m, Digital Instruments, Veeco Metrology Group) was used at a frequency in the range of 5.0−9.5 kHz. Cantilever, fluid cell, and Pt electrodes were carefully rinsed in turn with ethanol and water and then were dried with nitrogen before use. Electrochemical reactions and TMAFM imaging were performed intermittently during the experiment. For each experiment, at least five different areas were randomly chosen for imaging. The height and phase images were simultaneously recoded during AFM imaging.

Ex-Situ Degassing. After electrochemically generated nanobubbles were observed via TMAFM, the HOPG was carefully placed in a desiccator and was degassed by a vacuum pump (Shanghai Two Penguin Refrigeration Instrument Co., Ltd., Shanghai, China) at 0.1 atm for at least 2.5 h.

Results and Discussion

Evidence of Gas Nanobubbles. In this work, HOPG served both as the working electrode and the substrate for bubble formation. Bare HOPG provides an atomically flat and conveniently refreshable surface with reasonable hydrophobicity.[37] It is also an excellent conducting electrode material. Figure 1a showed a typical cyclic voltammetric (CV) curve recorded at a scan rate of 0.2 V/s (second cycle) and in 0.01 M H_2SO_4. By applying sufficiently negative potentials (< −1.2 V) on HOPG in a diluted sulfuric acid solution, abundant hydrogen gas was produced at the HOPG surface. After applying a voltage of −1.5 V for 10 s, we imaged the HOPG surface with TMAFM and observed the formation of spherical-cap nanobubbles via both height and phase images (Figure 1b and 1c). These nanobubbles were fairly stable, with little variations in both morphology and distribution over the experimental period (up to several hours). We also observed that nanobubbles were preferentially formed near atomic steps of HOPG and that the growth of nanobubbles was limited by two proximal atomic steps (see Figure 2c). This observation coincides well with the study of Compton and co-workers. They recently undoubtedly demonstrated that electrochemical reactions only occurred at edge-plane physical steps.[38] The basal-plane graphite, while occupying more than 99.5% of the total HOPG surface area, is effectively electrochemically inert.[38] Therefore, this consistency strongly supports that the observed nanobubbles were electrochemically generated.

Phase image in TMAFM is very sensitive to variations of material properties such as elasticity, adhesion, and viscoelasticity. Indeed, the electrochemically generated features showed similar phase contrast to that reported in nonelectrochemical conditions in the literature.[15,39,40] The large phase shifts over those features during phase imaging (shown in Figure 1c) suggested that these spherical-cap features were significantly different in nature from the "hard" HOPG surface and were indeed "soft" materials.[41] Moreover, similar to previous reports on nanobubbles,[15,40] the observed features could be manipulated by the AFM tip. After applying a voltage of −2.1 V for 2 s, we scanned a square area of 800 nm × 800 nm several times with increased tapping force (tip perturbation), and then the same region was rescanned with normal tapping force in an expanded scan window of 2.0 μm × 2.0 μm. Significantly, we observed the appearance of a big bubble in the square region (Figure 1d and 1e). This result suggests that the tip movement at increased tapping force could induce the fusion of several small nanobubbles into a big one.

To further confirm the existence of nanobubbles and distinguish nanobubbles from artifacts and contaminates, we employed a powerful technique, ex-situ degassing. We placed an HOPG with surface-confined nanobubbles in the desiccator and extensively degassed it. After this degassing process, we found that only very few nanobubbles, if any, existed in the same surface area (see Figure 2-S in the Supporting Information). In contrast, the nanobubble features on the HOPG surface were not significantly altered when the HOPG was placed in the desiccator without being degassed. Note that nanobubbles of gas origin can be

(29) Evans, D. R.; Craig, V. S. J.; Senden, T. J. *Physica A* **2004**, *339*, 101−105.
(30) Considine, R. F.; Drummond, C. J. *Langmuir* **2000**, *16*, 631−635.
(31) Zhang, J. H.; Yoon, R. H.; Mao, M.; Ducker, W. A. *Langmuir* **2005**, *21*, 5831−5841.
(32) Lugli, F.; Hofinger, S.; Zerbetto, F. *J. Am. Chem. Soc.* **2005**, *127*, 8020−8021.
(33) Ljunggren, S.; Eriksson, J. C. *Colloids Surf., A* **1997**, *130*, 151−155.
(34) Haupt, B. J.; Senden, T. J.; Sevick, E. M. *Langmuir* **2002**, *18*, 2174−2182.
(35) Meyer, E. E.; Lin, Q.; Israelachvili, J. N. *Langmuir* **2005**, *21*, 256−259.
(36) Doshi, D. A.; Watkins, E. B.; Israelachvili, J. N.; Majewski, J. *Proc. Natl. Acad. Sci. U.S.A.* **2005**, *102*, 9458−9462.
(37) Zhang, X. H.; Zhang, X. D.; Lou, S. T.; Zhang, Z. X.; Sun, J. L.; Hu, J. *Langmuir* **2004**, *20*, 3813−3815.
(38) Davies, T. J.; Hyde, M. E.; Compton, R. G. *Angew. Chem., Int. Ed.* **2005**, *44*, 5121−5126.
(39) Zhang, X. H.; Wu, Z. H.; Zhang, X. D.; Li, G.; Hu, J. *Int. J. Nanosci.* **2005**, *4*, 399−407.
(40) Simonsen, A. C.; Hansen, P. L.; Klösgen, B. *J. Colloid Interface. Sci.* **2004**, *273*, 291−299.
(41) Magonov, S. N.; Elings, V.; Whangbo, M. H. *Surf. Sci.* **1997**, *375*, L385−L391.

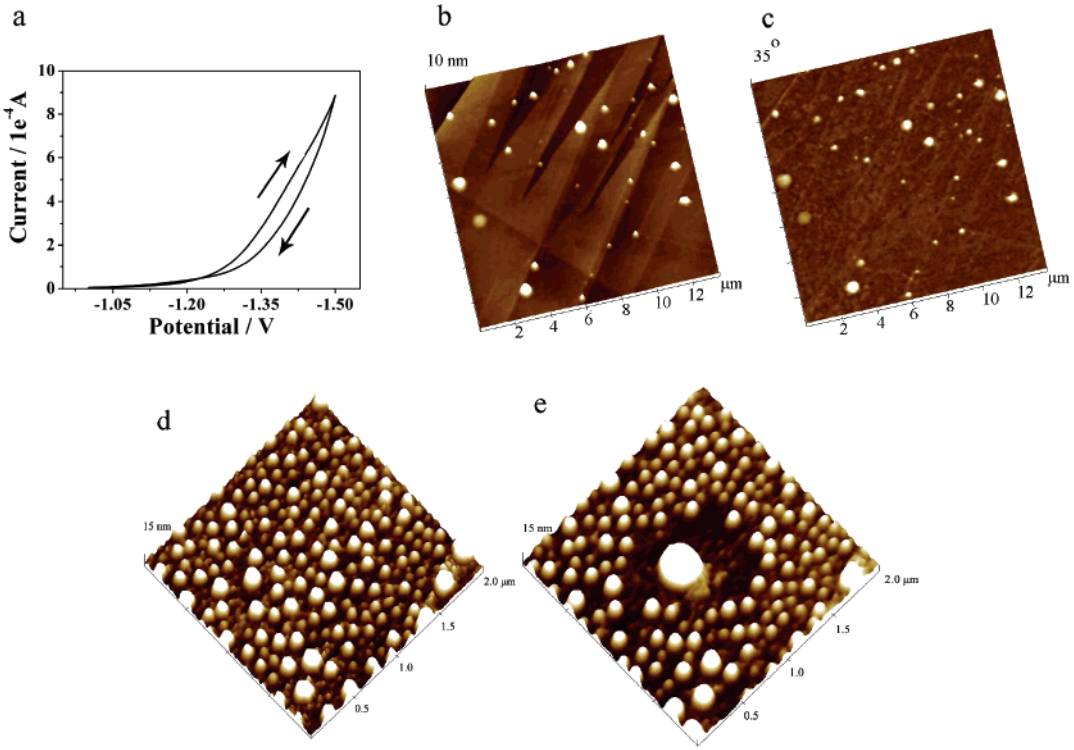

Figure 1. CV and AFM images. (a) A typical CV curve recorded at a scan rate of 0.2 V/s (second cycle) and in 0.01 M H_2SO_4. Hydrogen evolution begins at approximately −1.2 V. (b) Height and (c) phase images of electrochemically generated nanobubbles (light spherical-cap features) on HOPG surface after applying a voltage −1.5 V for 10 s. TMAFM images of nanobubbles obtained after applying a voltage of −2.1 V for 2 s (d) before and (e) after tip perturbation.

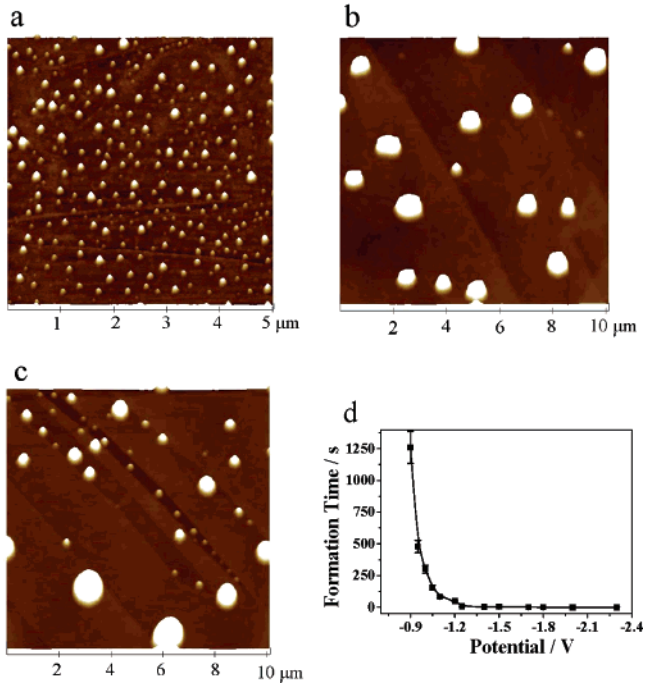

Figure 2. Dependence of nanobubble formation on applied voltage. Nanobubbles formed at a voltage of (a) −2.0 V for 5 s, (b) −1.4 V for 20 s, and (c) −1.8 V for 2 s. (d) Plot of the time for nanobubble formation versus the applied voltage. There was a voltage threshold about the formation of nanobubbles. *Z* range: 25 nm.

removed from the surface during the degassing process while other bubblelike features (artifacts) cannot with this technique.[37,42] This clearly confirmed that the nanobubble features were indeed gas bubbles while not artifacts or contaminations.

(42) Lubetkin, S. D. *Langmuir* **2003**, *19*, 2575−2587.

Controlled Formation of Nanobubbles. The formation of nanobubbles could be controlled by varying either the applied voltage or the reaction time. Figure 2a−c demonstrated several representative dimensional distributions of electrochemically generated nanobubbles on the HOPG surface. A large number of small nanobubbles were formed at a voltage of −2.0 V (see Figure 2a); fewer but bigger nanobubbles were produced at a voltage of −1.25 ∼ −1.8 V as shown in Figure 2b and c. Figure 2d showed the curve of time required for nanobubble formation versus the applied voltage, which was obtained by successive scanning of the surface after each voltage was applied for a certain reaction time. It was found that there was a voltage threshold of approximately −1.2 V about the formation of nanobubbles, which coincided well with the hydrogen evolution potential as indicated in the corresponding CV (Figure 1a). Below this threshold, we could only observe very scarce nanobubbles even after a long period (minutes to hours). Above this voltage, we observed the formation of a large number of nanobubbles on the time scale of seconds (Figure 2a−c). Generally, the higher the voltage, the greater the number and the smaller the size of nanobubbles produced. The apparent height and lateral width of such nanobubbles were ∼1.5−95 nm and ∼45−1600 nm (the tip convolution effect had been included), respectively.

Evolution of Nanobubbles on HOPG Electrode Surface. As a step further, we studied the dynamic process of nanobubble formation by continuously monitoring the evolution of electrochemically generated nanobubbles on the HOPG electrode surface. No nanobubble was observed in the absence of applied voltage (Figure 3a). Nanobubbles began to form after applying a voltage of −1.5 V for 4 s, and both the number and the height of nanobubbles increased with the reaction time within approximately 10 s (Figure 3b and 3c). The height data of nanobubbles could be obtained by analyzing images in Figure 3b−d using the "particle analysis" tool of the AFM offline

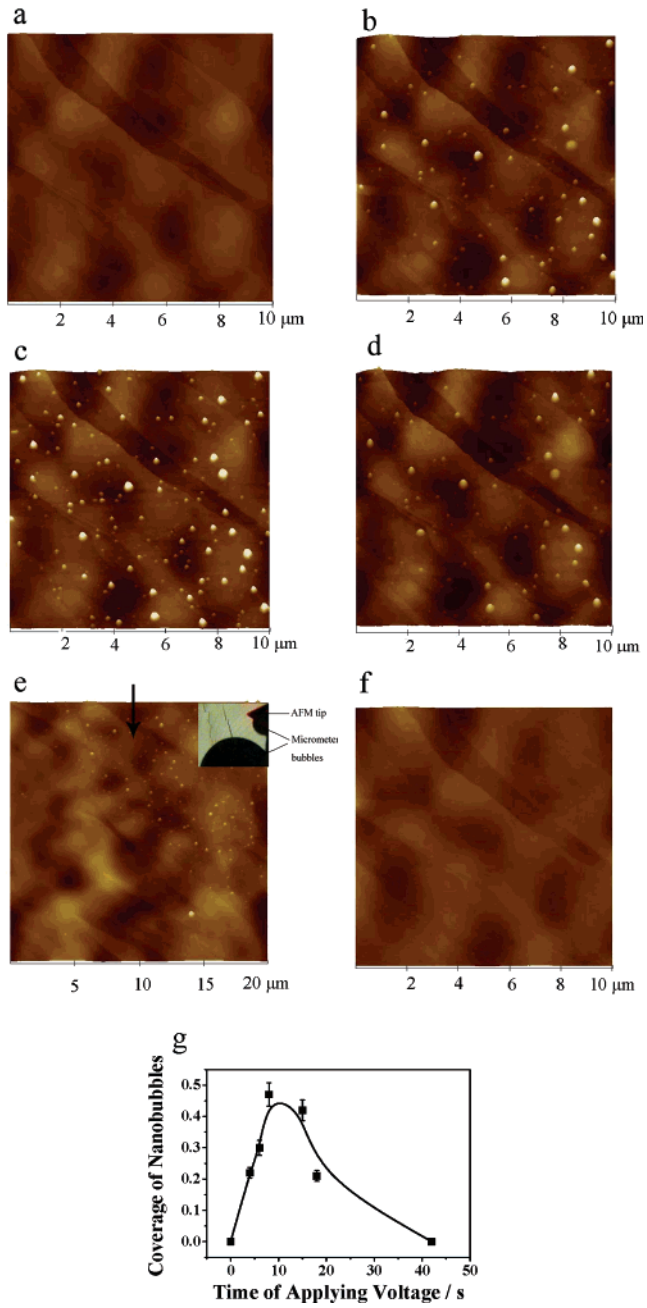

Figure 3. TMAFM images of nanobubbles and their evolution process on HOPG surface with the reaction time at a constant applied voltage. (a) Before applying voltage and after applying −1.5 V for (b) 4 s, (c) 8 s, and (d) 18 s. (e) The image of the enlarged area and a large bubble emerging near the tip (inset); the corresponding imaged region is indicated by arrow. (f) The image obtained after a large bubble emerging under the tip when the reaction time reached 43 s. (g) Plot of surface coverage of nanobubbles vs reaction time at the applied voltage of −1.6 V. *Z* range: 25 nm.

software. The average height of nanobubbles in Figure 3b−d was 8.9, 12.5, and 7.0 nm, respectively. The corresponding nanobubbles' numbers were 107, 161, and 98, respectively. Interestingly, further electrolysis (>10 s) reversed the process and decreased the number of nanobubbles (Figure 3d and 3e). This phenomenon might be associated with the coalescence of nanobubbles and the eventual release of merged microbubbles. In fact, we found an empty place in the imaged area (Figure 3e), and a micrometer-sized bubble appeared near the AFM tip at 18 s from the optical enlarged display (inset of Figure 3e). In addition, we found that tens of micrometer-sized bubbles emerged under the tip at 43 s. At this stage, we could no longer observe any nanobubble in the same area of the surface (Figure 3f). These phenomena suggested that the release of microbubbles caused the disappearance of nanobubbles in the imaged area. These results suggest that nanobubbles underwent an evolution process of formation, growth, and coalescence of nanobubbles and the eventual release of microbubbles. We could always reproduce the whole evolution process as demonstrated in the representative graph of surface coverage of nanobubbles versus reaction time (Figure 3g). Coverage of nanobubbles was defined as the ratio of the contact areas of nanobubbles formed on the surface to the calculated total areas. The contact areas of nanobubbles were obtained by the "particle analysis" tool of the AFM offline software. The monitoring of the evolution process undoubtedly confirmed the existence of gas nanobubbles.

On the basis of these observations, we propose a possible mechanism for the nanobubble evolution at the HOPG electrode. Initially, protons were reduced to hydrogen gas at physical steps of HOPG at a voltage < −1.2 V, which led to the formation of nanoscale bubbles. Nevertheless, the formation of these nanobubbles blocked further water electrolysis at these sites. This is consistent with the results of Nagai et al.,[43] who observed that the efficiency of water electrolysis decreased under high current densities. As a result, further electrolysis did not favor the increase of the number of nanobubbles; instead, nanobubbles began to grow and merge, leading to the formation of micrometer-sized bubbles and to their eventual release from the surface. The release of these microbubbles led to a bubble-free area where electrochemical reaction could take place again.

While we provided strong evidence that nanobubbles existed at the HOPG electrode surface, we note that this conclusion could not be simply extended to other systems. That is, the confirmation of nanobubble existence at the electrochemical interface does not necessarily mean that nanobubbles universally exist at solid−liquid interfaces.[44] It is important to point out that a large amount of gas was produced in the vicinity of the HOPG surface and that the gas source was solely electrochemically generated hydrogen in the present system. In contrast, most previously investigated systems usually involved complex gas composition and relatively limited gas supply.[9−12,15]

Interrogation of nanobubbles at the electrochemical interface contributes to probing the "nanobubble mystery".[45] Moreover, the formation and stable existence of hydrogen nanobubbles at the electrode surface might be responsible for various existing electrochemical phenomena, such as the increase of ohmic resistance[46] and overvoltage[47] proximal to the electrode, the origin of bubble-shaped defects or heterogeneous coating in electrochemical etching or electrodeposition,[2,3] hydrogen embrittlement of metals and alloys during electroplating, and cathodic protection and corrosion of metals.[48] Given that nanobubbles may exist at the electrode surface, it is necessary to revisit the mechanisms of these widely existing phenomena. In addition, the controlled formation and growth of nanobubbles might offer some new insights in the development of new techniques. For instance, electrogenerated nanobubbles can be used as valves in nanofluid

(43) Nagai, N.; Takeuchi, M.; Kimura, T.; Oka, T. *Int. J. Hydrogen Energy* **2003**, *28*, 35−41.
(44) Meyer, E. E.; Lin, Q.; Hassenkam, T.; Oroudjev, E.; Israelachvili, J. N. *Proc. Natl. Acad. Sci. U.S.A.* **2005**, *102*, 6839−6842.
(45) Wu, Z. H.; Zhang, X. H.; Zhang, X. D.; Li, G.; Sun, J. L.; Zhang, Y.; Li, M. Q.; Hu, J. *Surf. Interface Anal.* **2005**, *37*, 797−801.
(46) Bongenaar-Schlenter, B. E.; Janssen, L. J. J.; van Stralen, S. J. D. *J. Appl. Electrochem.* **1985**, *15*, 537−548.
(47) Monev, M.; Mirkova, L.; Krastev, I.; Tsvetkova, H.; Rashkov, S.; Richtering, W. *J. Appl. Electrochem.* **1998**, *28*, 1107−1112.
(48) Coleman, D. H.; Popov, B. N.; White, R. E. *J. Appl. Electrochem.* **1998**, *28*, 889−894.

chips[49] or as templates to prepare nanoscale containers or crystals.[7,50] The formation of high coverage of hydrogen nanobubbles on graphite surfaces may also lead to a novel hydrogen-storage method.[51]

Conclusion

In this work, we established a well-defined system that could produce a large amount of single component gas, hydrogen by electrolysis of diluted sulfuric acid at the HOPG electrode. In our experiments, the existence of hydrogen nanobubbles was demonstrated by both phase image and perturbation of the AFM tip and was further confirmed by the ex-situ degassing method. We observed that there was a voltage threshold for the appearance of nanobubbles and that the formation and growth of nanobubbles could be well controlled by tuning the applied voltage and the reaction time. We also in situ monitored the whole evolution process of nanobubbles, that is, formation, growth, and coalescence of nanobubbles as well as eventual release of merged microbubbles from the surface.

Acknowledgment. We thank Prof. Ruhong Zhou for helpful discussion. We gratefully appreciate financial support from the National Natural Science Foundation of China (10335070, 60537030, 10474109), the Chinese Academy of Sciences, the Shanghai Municipal Commission for Science and Technology Commission (0552 nm033, 03DZ14025), Shanghai Rising-Star Program, and the Ministry of Science and Technology of China.

Supporting Information Available: Detailed description of experiments and additional data. This material is available free of charge via the Internet at http://pubs.acs.org.

LA060859F

(49) Hua, S. Z.; Sachs, F.; Yang, D. X.; Chopra, H. D. *Anal. Chem.* **2002**, *74*, 6392−6396.
(50) Bajpai, V.; He, P. G.; Dai, L. M. *Adv. Funct. Mater.* **2004**, *14*, 145−151.
(51) Chambers, A.; Park, C.; Baker, R. T. K.; Rodriguez, N. M. *J. Phys. Chem. B* **1998**, *102*, 4253−4256.